Journal of Aeronautical
-Science and Engineering-, Vol.14

May 30, 2018

Numerical Analysis of the Effect of Microriblet on the Lift and Drag of the WIG

Alireza Heidarian,[a,*] and Hassan Ghassem,[b]

[a)]*Department of Marine Engineering, Persian Gulf University, Boushehr, Iran*
[b)]*Department of Maritime Engineering,Amirkabir University of Technology, Tehran, Iran*

*Corresponding author: gasemi@aut.ac.ir

Paper History

Received: 15-April-2018
Received in revised form: 20-May-2018
Accepted: 30-May-2018

ABSTRACT

Engineering marvels have led to the design and build the wing-in-ground (WIG) craft to fill the gap between ships and aircraft as a new opportunity for transportation. One of the most significant issues in WIG craft are drag and lift force when the craft starting to plane. Living nature has been used to solve the mentioned challenge. There are various ways in nature to reduce drag force in fluid flow, such as the evidence in the movements of fish, sharks and dolphins, the skin of fast-swimming sharks is covered by microriblets that assist them to move fast. In this study, Computational Fluids Dynamics (CFD) method is implemented to the investigation the influence of microriblet film on aerodynamic of the WIG craft. A Clark-Y wing was simulated in ANSYS CFX simulation software at various Reynolds number to investigate the effects of riblets on aerodynamic characteristics of the wing in ground effects.

KEY WORDS: *WIG craft; CFD method; Clark-Y Wing; Riblet; Drag reduction; Lift growth.*

1.0 INTRODUCTION

The wing-in-ground-effect (WIG) craft bridge between aircraft and water craft. The speed of WIG craft is higher than a traditional fast boat and its efficiency is greater than an aircraft. The low fuel consumption of WIG craft in cruise mode is an excellent economic option compared to aircraft. This advantage makes the WIG craft to have long flight endurance. The flow behaviour around a wing is substantially influenced by the ground effect. The stagnation point shifts to the lower side of the wing and leads to a larger part of the air diverting over the wing [1]. Therefore, the speed of the air at the lower side of the wing reduces and hence it raises the pressure and accordingly, a dynamic air cushion is created. For a very low ground clearance, large pressure is generated at the pressure side; named as ram pressure, as the lift obtains a noticeable enhancement. Concurrently, the downwash velocity reduces and causes a drop in induced drag [2]. The effective aspect ratio of the wing in proximity to the ground is greater than a geometric one [3]. Two phenomena influence the aerodynamic characters of wing when the wing approaches the ground. These are called span dominated and chord dominated ground effect. The main parameter related to span dominated ground effect is h/b (height-to-span ratio) and for chord dominated ground effect is h/c (height-to-chord ratio). Many researchers have made some efforts to develop WIG craft to fly near the ground. The earlier researches in the development of WIG craft were carried out in Finland, Russia, Sweden and the United States [4]. Recently, many countries started to work and develop WIG craft because of their advantages such as fuel saving and high speed compared to other water vehicles. The studies on the configuration of WIG craft experimentally and theoretically have been made to improve their aerodynamic performance. The principal means to develop lifting force is the ram effect; lift is improved when the flow underneath the wing body around stagnation point on the pressure surface (lower surface of body) is trapped. The gathering of high pressure on the lower surface and low pressure on the upper surface of the body produces a high lifting force which increases the source of support. Chun and Chang numerically investigated the turbulent flow of the wing with and without considering the effects of the ground [5]. An incompressible Reynolds Average Navier-Stokes (RANS) equation with finite difference method was applied in their numerical model. According to their computational results, the type of ground model does not have much effect on the lift

JAse | Received: 15-April-2018 | Accepted: 30-May-2018 | [(14) 1: 5-10]
Published by International Society of Ocean, Mechanical and Aerospace Scientists and Engineers, www.isomase.org., ISSN: 2442-6407

and moment coefficients, but the predicted drag coefficients with the fixed bottom were slightly smaller than the moving ones. Zerihan and Zhang numerically analysed the pressure distribution and wake region around a single element and was validated by experimental data [6]. A Reynolds-averaged Navier–Stokes (RANS) was exercised for 2D simulation with structured grid, and the SST k-w and Saplart-Allmaras turbulence models were employed for turbulent flow around the wing. Telenta et al demonstrated that SST k-w and realizable k-ε turbulence models are suitable for estimating the pressure distributions and visualization of wake region, respectively. They used multi block hybrid grids. Also, the standard k-ε turbulence model was applied for a racing car wing [7]. The flow structure under the suction surface of the invert wing is constrained with ground level. The flow considerably accelerates as the wing approaches with proximity to the ground which results in higher suction and consequently greater downforce as compared with freestream. The greater downforce may lead to the separation of the fluid at the rear of suction surface. Using shark's riblets is deemed to be better solution to destroy the effects of the separation on wing in the ground effect [8]. The riblet on the surface of fast swimming sharks decreases the drag as they move through the water [9].

The small scales covering the skin of fast-swimming sharks, identified as dermal denticles (skin teeth) are formed like small riblets and arranged in the direction of fluid flow. Riblets are useful for drag reduction of objects where the drag is caused by turbulent flow, where on the objects with fairly flat edges [11].

2.0 DRAG REDUCTION BY SHARK'S RIBLET

The compliant skin of dolphins has been studied for drag reduction capabilities, and showed to be useful by responding to the pressure fluctuations across the surface [12]. Riblets are beneficial for drag reduction of objects where the drag is caused by turbulent flow, thus suitable for the long objects with fairly flat edges. Riblets are not effective on objects with pressure drag as their dominant drag force [13]. Geometry of riblets includes blade, saw tooth, scalloped, and bull nose with continuous and segmented configurations (aligned and staggered). Typical geometries of saw tooth, scalloped and blade riblets are shown in Figure 2 [14].

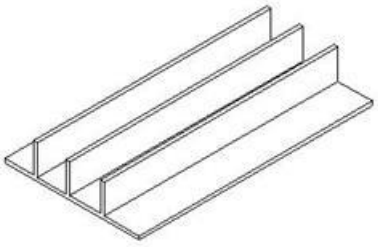

Figure 1. Blade microriblet

In turbulent conditions where the fluid molecules move in nonparallel directions and thus cross flow velocities exist between the molecules, a noticeable increase in momentum transfer will occur. This increase is of high significance because any momentum transfer parallel to the object surface will increase drag. Riblets, the small pieces covering the increased drag in turbulent flow by decreasing the momentum transfer. This is possible by the elevation of the vortices above the surface and prevention of the cross-stream movement of the stream-wise vortices in the viscous sublayer [15]. The use of riblet for the purpose of drag reduction does not seem obvious at the beginning, because it increases the total wetted area, thus increases the drag due to the rise in the shear stress [16]. But, another mechanism appears here, which is the lifting of the vortices by the riblets. What happens is that riblets shift the formed vortices to the riblet tips region and fluid with lower velocity will flow between the tips. Therefore, the vortices interaction is only with the small surface of the tips and high shear stress happens in this small area whereas the large area between the tips experiences a slight shear stress caused by the low velocity flow. When the vortices are kept above the tips, the fluctuations of the cross stream velocity between the riblets are much lower than that above of the aerofoil. Therefore, the shear stress and momentum transfer is lower near a riblet covered surface, which reduces the effect of increased area due to the riblets [17].

3.0 NUMERICAL ANALYSIS

A simulation was done using the ANSYS design modeller software [18]. The computational geometry is shown in Figure 3. A Clark-Y aerofoil was used which has a chord length of 7.5 cm and a span of 10 cm. In this study, the aerofoil was simulated by film with and without microriblets. The foil with and without microriblets was placed in a fluid flow at various velocities. The dimensions of the riblet that applied on the aerofoil are $h = 162\mu m, s = 340\mu m$ and are shown in Figures 4. For 5 different speeds, principal aerodynamic characteristics were compared between the plain (no riblet) and ribleted aerofoil. Figure 3 shows the physical domain of simulation. To simulate ground effects, the bottom wall is set to move with the inlet surface.

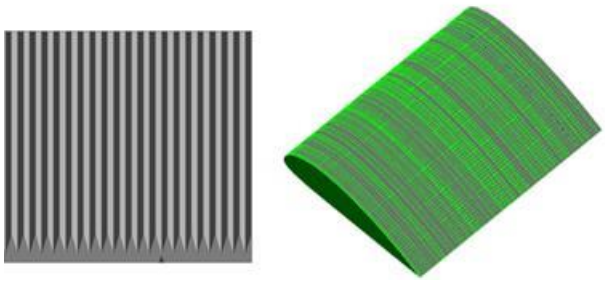

Dimension of riblets Microriblets applied on the aerofoil's surface

Figure 2. The size of riblets applied on aerofoil's surface

3.1 Meshing

A simulation was made by various number of mesh elements and eventually the optimum value of mesh is selected based on y^+ values. Five different meshes representing coarse (850,214 nodes), medium (2,053,680 nodes), fine (4,238,573), very fine (7,464,312 nodes) and ultrafine (10,464,312) were examined to select the best mesh size for the riblets based on the maximum y^+

JAse | Received: 15-April-2018 | Accepted: 30-May-2018 | [(14) 1: 5-10]
Published by International Society of Ocean, Mechanical and Aerospace Scientists and Engineers, www.isomase.org., ISSN: 2442-6407

and predicted drag coefficient. The drag coefficient changes from the coarse mesh to the ultrafine mesh, where an acceptable maximum $y^+ = 18$ is achieved. This value assures that the boundary layer can be fairly well resolved. An inflation was considered around the aerofoil and the size of mesh was changed. By using 7.4 million nodes the predicted drag coefficient reached 0.211902 and after introducing the inflation by the first layer height of 5e-4, about 10 million elements were acquired and the predicted drag coefficient reached 0. 21119 (about 0.5 percent difference). Therefore, the very fine mesh was selected for the simulations.

4.0 RESULTS AND DISCUSSION

Plots in Figure 5 show numerically simulated flow over an aerofoil without and with riblet on top of the surface. Values of drag reduction are based on the Reynolds number. The diagram reveals that the drag coefficient of the ribleted aerofoil is less than a simple plate. The graph in Figure 5 compares the values of drag coefficient based on Reynolds number for the ribleted aerofoil and plain aerofoil. It shows that by increasing the speed, the drag coefficient is reduced and the maximum amount of drag reduction of ribleted aerofoil in comparison with the plain aerofoil is 7%.

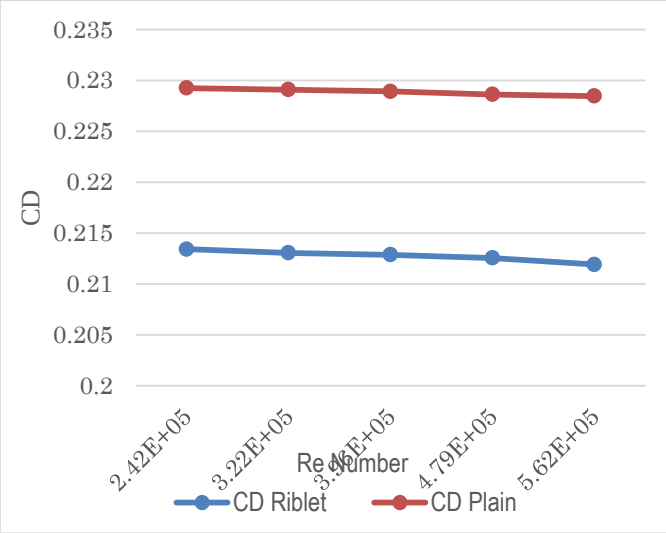

Figure 3. Drag coefficient based on the Reynolds number for the plain and riblet aerofoil at different velocities

Based on the Figure 6, the lift coefficient of the ribleted aerofoil is higher than the plain aerofoil in different velocities and it is because of the effects of riblets on vortex around the aerofoil. The riblets have some strong effect on the lift production due to vortices.

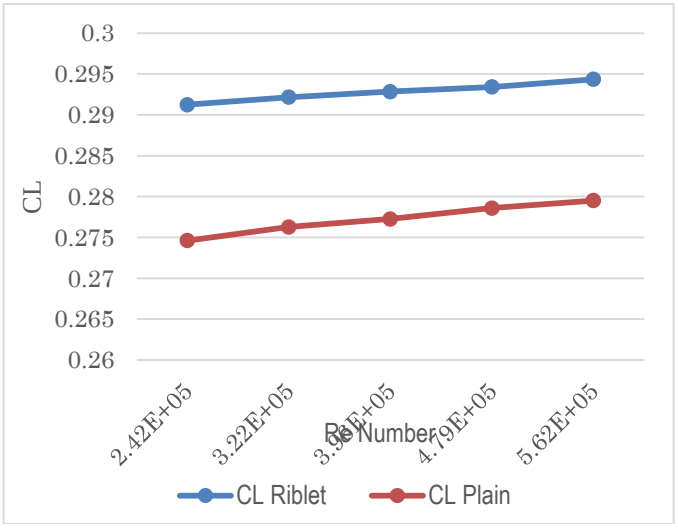

Figure 4. Lift coefficient on the Reynolds number plain and microriblet aerofoil at different velocities

What happens is that the riblets shift the formed vortices towards the riblet tips and the fluid with lower velocity will flow between the tips [19]. Therefore, the interaction of vortices is only with the small surface of the tips and hence high shear stress acting on this small area whereas the large area between the tips experiences a slight shear stress caused by the low velocity flow. When the vortices are kept above the tips, the fluctuations of the cross stream velocity between the riblets are much lower than that above a flat plate. Therefore, the shear stress and momentum transfer are lower near a riblet covered surface, which reduces the effect of increased area due to the riblets.

4.1 Pressure coefficient

The variation of the pressure coefficient (Cp) at the middle span on the surface of the rectangular wing was studied for the ground effect and is shown in Figure 7. The positive pressure on the lower surface and negative pressure (suction effect) on the upper surface of the wing increased when the microriblets are used. The pressure of the upper surface is lower than the lower surface. According to Figure 10 at 70m⁄s, the ribleted aerofoil created suction is higher than that of the plain aerofoil. Consequently, the aerofoil may start planning with higher suction pressure and hence energy consumption decreases. The flow considerably accelerates as the riblets applied on the aerofoil which results in a higher suction and is, therefore, greater downforce as compared with freestream.

JAse | Received: 15-April-2018 | Accepted: 30-May-2018 | [(14) 1: 5-10]
Published by International Society of Ocean, Mechanical and Aerospace Scientists and Engineers, www.isomase.org., ISSN: 2442-6407

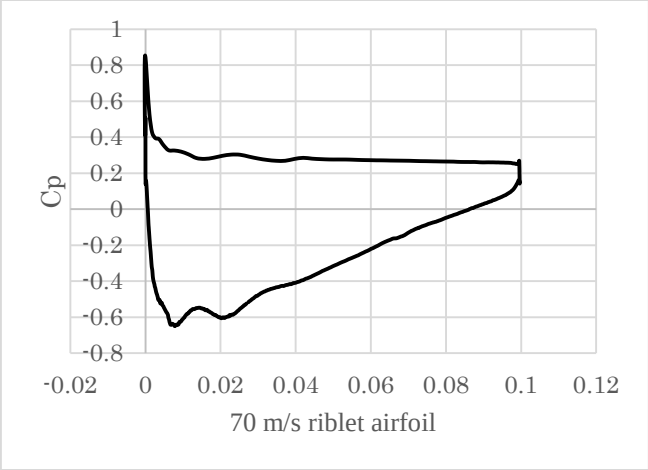

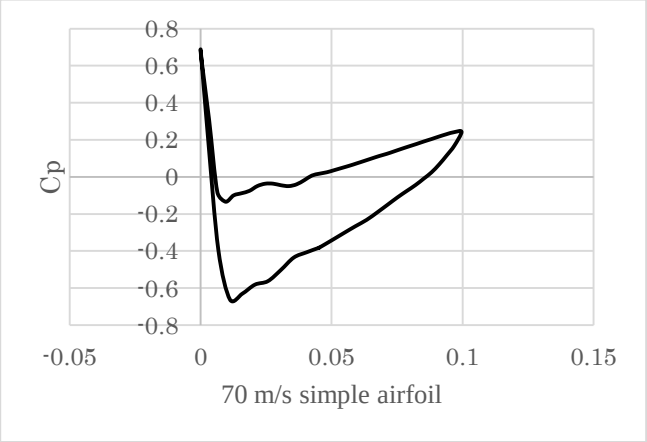

Figure 5. Pressure coefficient along the chord of the midsection of the microriblet and plain aerofoil

Based on Figure 7 the pressure difference between the upper and the lower surface of the ribleted aerofoil is higher than the plain simple aerofoil and it means that the ribleted aerofoil produced more lift force than the plain aerofoil.

4.2 Pressure Plots

Pressure contours in Figure 8 represent that at various velocities the pressure of the plain aerofoil is smaller than ribleted aerofoil. While pressure starts to increase, the wing can easily start to plane because the air pressure helps it to fly, but in the plain aerofoil, there is no auxiliary force and need higher energy to start flying. Consequently craft use plain foil surface would need an engine of larger power and thus it would increase the cost of production of the aircraft and higher operation cost. For the ribleted aerofoil the stagnation point would be placed at the lower position than plain aerofoil and therefore the sensitive areas of the wing, especially at the leading edge of the aerofoil receives lower force than that of the plain aerofoil.

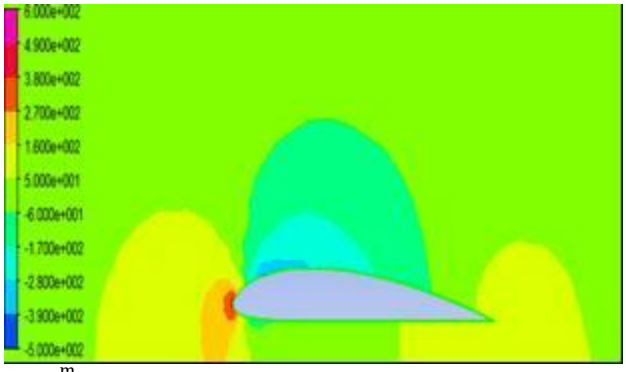

V=30$\frac{m}{s}$ Plain aerofoil

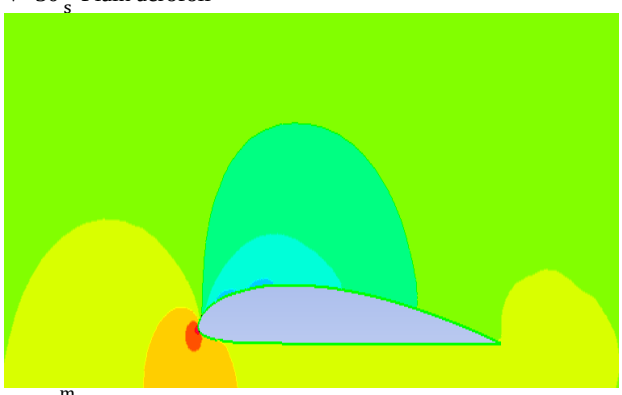

V=30$\frac{m}{s}$ riblet aerofoil

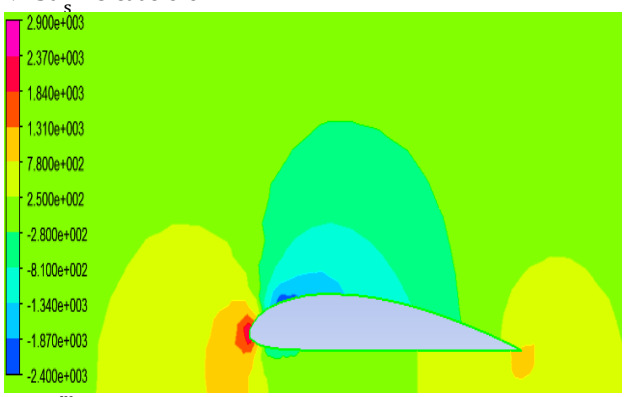

V=70$\frac{m}{s}$ Simple aerofoil

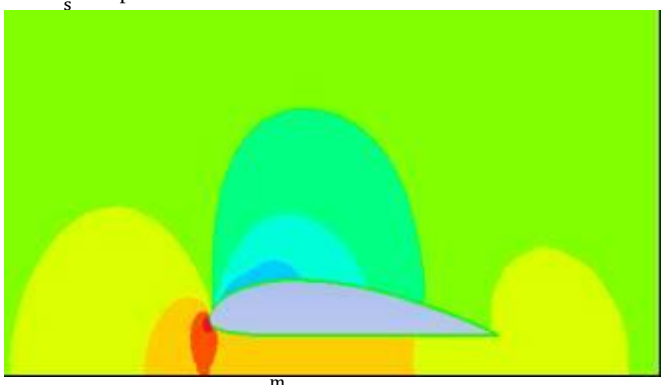

V=70$\frac{m}{s}$ Riblet aerofoil

Figure 6. Pressure contours for different velocities

JAse | Received: 15-April-2018 | Accepted: 30-May-2018 | [(14) 1: 5-10]
Published by International Society of Ocean, Mechanical and Aerospace Scientists and Engineers, www.isomase.org., ISSN: 2442-6407

4.3 Velocity plots

Velocity contours of ribleted aerofoil and plain aerofoil are shown in Figure 9. Based on the figure, the separation on the ribleted aerofoil is delayed compared to the plain aerofoil. It means that the major parts of aerofoil have smaller pressure and the force due to the reduction of fluid separation and lift force are increased at similar velocities. The bottom of the ribleted aerofoil has smaller velocity and thus higher pressure compared with that of the plain aerofoil.

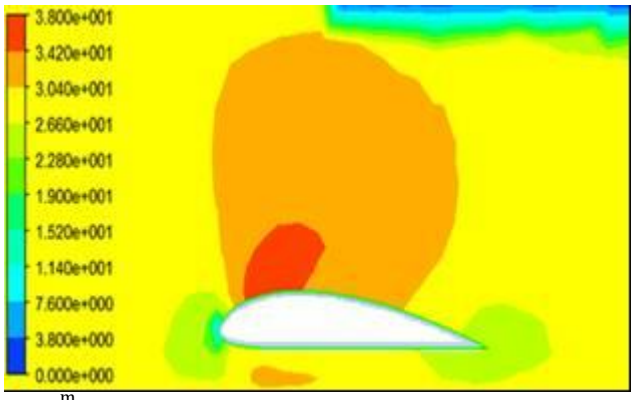

V=30$\frac{m}{s}$ plain aerofoil

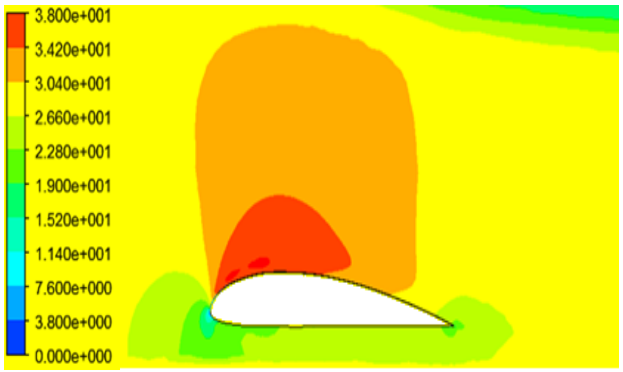

V=30$\frac{m}{s}$ Ribleted aerofoil

V=70$\frac{m}{s}$ Plain aerofoil

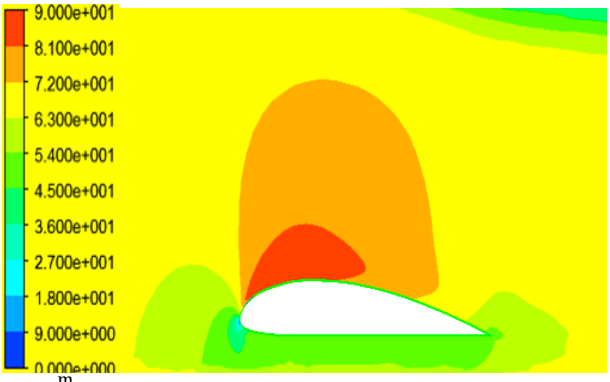

V=70$\frac{m}{s}$ Ribleted aerofoil

Figure 7. Velocity contours of different velocities for microriblet and plain aerofoil

The velocity contours in Figure 9 show that the separation on the plain aerofoil is more likely than ribleted aerofoil, which means that the major parts of the wing have smaller pressure and the force due to fluid separation decreases and the lift force increase in similar velocities. For aerofoils sometimes the separation occurs near the leading edge and hence it gives a growth to a short bubble. Separation can be dangerous especially towards the trailing edge where the flow is not reattached. In this situation, the separated region merges with the wake and may result in a stall. Using microriblet film makes flow to be more aberrant. Turbulent flow has more energy and momentum than laminar flow and hence it may eliminate separation and the flow may reattach. A short bubble may not be of much concern. The bottom of the ribleted wing has a lower velocity compared with that of the plain aerofoil, which, in conclusion, has a higher pressure. The separation in the boundary layer may lead to an enhancement of the displacement thickness which lessens the potential of fluid flow.

5.0 CONCLUSION

The reduction of skin friction in aviation industry helps to save fuel, which is a positive aspect for the environment and hence the reduced costs for operation. One promising way to decrease skin friction is to structure surfaces with riblets. This research numerically investigated the effects of shark's riblets on aerodynamics parameters of the aerofoil in air, for different Reynolds numbers. In this research, riblets are simulated in ANSYS CFX. The present research numerically studied the physics of the flow around a Clark-Y wing section for WIG craft at different velocities. Results reveal that skin friction drag is effectively reduced by using riblets, especially through lifting turbulent vortices. Effects of transverse shear stress and momentum transfer are minimized by vortices lifting. Experimental data using riblets of 3M Company were compared with the present numerical results. Based on the predicted results, ribleted aerofoil has a higher drag reduction of about 8%aerofoil. By comparing the drag coefficients of the plain and ribleted flat plates it is concluded that riblets can reduce drag force about 7% and increase lift production of force about 6%. The recorded

JAse | Received: 15-April-2018 | Accepted: 30-May-2018 | [(14) 1: 5-10]
Published by International Society of Ocean, Mechanical and Aerospace Scientists and Engineers, www.isomase.org., ISSN: 2442-6407

positive pressure on the lower surface of the ribleted wing was noticeably stronger than that of the plain wing. However, the suction effect on the upper surface of the plain wing was slightly higher.

REFERENCE

1. Abdel Wahab, M., et al., Experimental and Numerical Investigation of Flutter Phenomenon of an Aitcraft Wing (Naca 0012). Mechanics, 2017. 23(4).
2. Yang, W., Z. Yang, and C. Ying, Effects of design parameters on longitudinal static stability for WIG craft. International Journal of Aerodynamics, 2010. 1(1): p. 97-113.
3. Jia, Q., W. Yang, and Z. Yang, Numerical study on aerodynamics of banked wing in ground effect. International Journal of Naval Architecture and Ocean Engineering, 2016. 8(2): p. 209-217.
4. Qu, Q., et al., Numerical study of the aerodynamics of a NACA 4412 airfoil in dynamic ground effect. Aerospace Science and Technology, 2014. 38: p. 56-63.
5. Jung, J.H., et al., Mean flow characteristics of two-dimensional wings in ground effect. International Journal of Naval Architecture and Ocean Engineering, 2012. 4(2): p. 151-161.
6. Zerihan, J. and X. Zhang, A single element wing in ground effect - Comparisons of experiments and computation, in 39th Aerospace Sciences Meeting and Exhibit. 2001, American Institute of Aeronautics and Astronautics.
7. Telenta, M., et al., Detached Eddy Simulation of the flow around a simplified vehicle sheltered by wind barrier in transient yaw crosswind. Mechanics, 2015. 21(3).
8. Lee, S.J. and Y.G. Jang, Control of flow around a NACA 0012 airfoil with a micro-riblet film. Journal of Fluids and Structures, 2005. 20(5): p. 659-672.
9. Viswanath, P.R., Aircraft viscous drag reduction using riblets. Progress in Aerospace Sciences, 2002. 38(6): p. 571-600.
10. Brian Dean, B.B., Shark-Skin Surfaces For Fluid-Drag Reduction in Turbulent Flow: A Review. Advances in Mechanics, 2012. 42(6): p. 821-836.
11. Bechert, D.W., et al., Fluid Mechanics of Biological Surfaces and their Technological Application. Naturwissenschaften, 2000. 87(4): p. 157-171.
12. Davies, C. and P.W. Carpenter, Instabilities in a plane channel flow between compliant walls. Journal of Fluid Mechanics, 1997. 352: p. 205-243.
13. Dean, B. and B. Bhushan, Shark-skin surfaces for fluid-drag reduction in turbulent flow: a review. Philosophical Transactions of the Royal Society of London A: Mathematical, Physical and Engineering Sciences, 2010. 368(1929): p. 4775-4806.
14. Zhao, D., et al., Study on the Hydrophobic Property of Shark-Skin-Inspired Micro-Riblets. Journal of Bionic Engineering, 2014. 11(2): p. 296-302.
15. Bixler, G.D. and B. Bhushan, Biofouling: lessons from nature. Philosophical Transactions of the Royal Society of London A: Mathematical, Physical and Engineering Sciences, 2012. 370(1967): p. 2381-2417.
16. Matin, A., N. Merah, and A. Ibrahim, Superhydrophobic and self-cleaning surfaces prepared from a commercial silane using a single-step drop-coating method. Progress in Organic Coatings, 2016. 99(Supplement C): p. 322-329.
17. Goldstein, D., R. Handler, and L. Sirovich, Direct numerical simulation of turbulent flow over a modeled riblet covered surface. Journal of Fluid Mechanics, 1995. 302: p. 333-376.
18. ANSYS CFX-Solver Theory Guide. 2011.
19. Shelley, S.R., et al., Fluid mobility over corrugated surfaces in the Stokes regime. Physics of Fluids, 2016. 28(8): p. 083101.
20. Harvey, W.D., International Pacific Air and Space Technology Conference, Melbourne, Australia, Nov. 13-17, 1987, Proceedings (A89-10627 01-01). Warrendale, PA, Society of Automotive Engineers, Inc., 1988, p. 287-311.

JAse | Received: 15-April-2018 | Accepted: 30-May-2018 | [(14) 1: 5-10]
Published by International Society of Ocean, Mechanical and Aerospace Scientists and Engineers, www.isomase.org., ISSN: 2442-6407